THE JOURNAL OF PHYSICAL CHEMISTRY A

Article

pubs.acs.org/JPCA

Bridging Gold in Electron-Deficient $Al_2Au_n^{0/-}$ and $BAlAu_n^{0/-}$ (n = 1−3) Clusters

Wen-Zhi Yao,*[,†] Bing-Tao Liu,[†] Zhang-Hui Lu,[‡] and Si-Dian Li[§]

[†]Department of Environmental and Municipal Engineering, North China University of Water Conservancy and Electric Power, Zhengzhou, 450011, China

[‡]College of Chemistry and Chemical Engineering, Jiangxi Normal University, Nanchang, 330022, China

[§]Institute of Molecular Science, Shanxi University, Taiyuan, 030001, China

ABSTRACT: The geometrical and electronic structures of the electron-deficient dialuminum aurides $Al_2Au_n^{0/-}$ and hybrid boron−aluminum aurides $BAlAu_n^{0/-}$ (n = 1−3) are systematically investigated based on the density and wave function theories. Ab initio theoretical evidence strongly suggests that bridging gold atoms exist in the ground states of C_{2v} Al_2Au^- ($^3B_1$), C_{2v} Al_2Au ($^2B_1$), C_{2v} $Al_2Au_2^-$ ($^2A_1$), C_{2v} Al_2Au_2 ($^1A_1$), C_s $Al_2Au_3^-$ ($^1A'$), and D_{3h} Al_2Au_3 ($^2A_1$), which prove to possess an Al−Au−Al τ bond. For $BAlAu_n^{0/-}$ (n = 1−3) mixed clusters, bridging B−Au−Al units only exist in C_s $BAlAu_3^-$ ($^1A'$) and C_s $BAlAu_3$ ($^2A'$), whereas C_s $BAlAu^-$ ($^3A''$), C_s $BAlAu$ ($^2A''$), C_s $BAlAu_2^-$ ($^2A'$), and C_s $BAlAu_2$ ($^1A'$) do not possess a bridging gold, as demonstrated by the fact that B−Al and B−Au exhibit significantly stronger electronic interaction than Al−Au in the same clusters. Orbital analyses indicate that Au 6s contributes approximately 98%−99% to the Au-based orbital in these Al−Au−Al/B−Au−Al interactions, whereas Au 5d contributes 1%−2%. The adiabatic and vertical detachment energies of $Al_2Au_n^-$ (n = 1−3) are calculated to facilitate future experimental characterizations. The results obtained in this work establish an interesting τ bonding model (Al−Au−Al/B−Au−Al) for electron-deficient systems in which Au 6s plays a major factor.

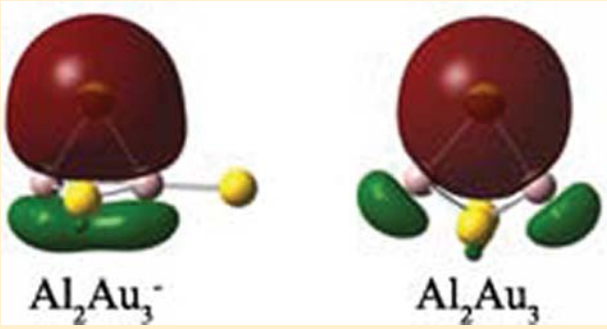

1. INTRODUCTION

Gold significantly differs from copper and silver in both physical and chemical properties mainly because of its strong relativistic effects: the stabilization and contraction of the 6s shell and the concomitant destabilization and expansion of the 5d.[1,2] These effects give rise to the high electronic affinity of Au, which behaves like halogens in alkaline and transition metal aurides.[1−4] Au also possesses the highest electronegativity (2.4) among all metals, which is comparable with that (2.2) of H. The surprising discovery of $H/AuPR_3$ analogy[5] and, more recently, H/Au analogy in $SiAu_4^{0/-}$,[6] $Si_2Au_x^{0/-}$ (x = 2, 4),[7] $B_7Au_2^{0/-}$,[8] and $B_nAu_n^{2-}$ (n = 5−12)[9] well supports the similarities between hydrogen and gold in terms of chemical bonding. Relativistic pseudopotential calculations on XAu_n^{m+} containing Au ligands (X = B−N, Al−S, n = 4−6) are also reported.[10] Our group recently present an ab initio investigation on diboron aurides $B_2Au_n^{0/-}$ (n = 1, 3, 5) and their $B_2H_mAu_n^-$ mixed analogues ($m + n$ = 3, 5),[11] monoboron aurides $BAu_n^{0/-}$ (n = 1−4) series,[12] and monoaluminum aurides $AlAu_n^{0/-}$ (n = 2−4).[13] These studies also confirmed the H/Au isolobal relationship and revealed a clear structural link between gold-containing clusters X_mAu_n and the corresponding hydride molecules X_mH_n. In most cases, gold serves as terminal atoms in conventional two-center two-electron (2c-2e) bonds in the reported compounds. However, in disilicon aurides $Si_2Au_x^{0/-}$ (x = 2, 4)[7] and diboron aurides $B_2Au_n^{0/-}$ (n = 1, 3, 5),[11] Au serves as bridging atoms in Si−Au−Si and B−Au−B three-center two-electron (3c-2e) interactions (τ orbitals). Given the fact that the H-bridged Al−H−Al unit is of essential importance in the well-documented dialane,[14] we try to determine whether Au can replace H to form Au-bridged Al−Au−Al in electron-deficient systems which are similar to diboron aurides $B_2Au_n^{0/-}$ (n = 1, 3, 5). Starting from the smallest aurodialane Al_2Au and the mixed analogues BAlAu, we performed a systematic ab initio investigation on $Al_2Au_n^{0/-}$ and $BAlAu_n^{0/-}$ (n = 1−3) in this work. Theoretical evidence based on both the density functional theory (DFT) and wave function theory strongly suggests that the ground-state $Al_2Au_n^{0/-}$ (n = 1−3) and $BAlAu_3^{0/-}$ contain bridging gold (Au_b) atoms in Al−Au−Al and B−Au−Al τ bonds. Al_2Au_n (n = 1−3) neutrals form Al−Au−Al bridging interactions similar to that in Al_2H_n (n = 1−3), whereas $BAlAu^{0/-}$ and $BAlAu_2^{0/-}$ do not possess bridging gold in their ground-state structures. The adiabatic (ADEs) and vertical electron detachment energies (VDEs) of $Al_2Au_n^-$ (n = 1−3) anions are calculated to aid their photoelectron spectroscopy (PES) characterizations. The

Received: March 17, 2013
Revised: May 29, 2013
Published: May 29, 2013

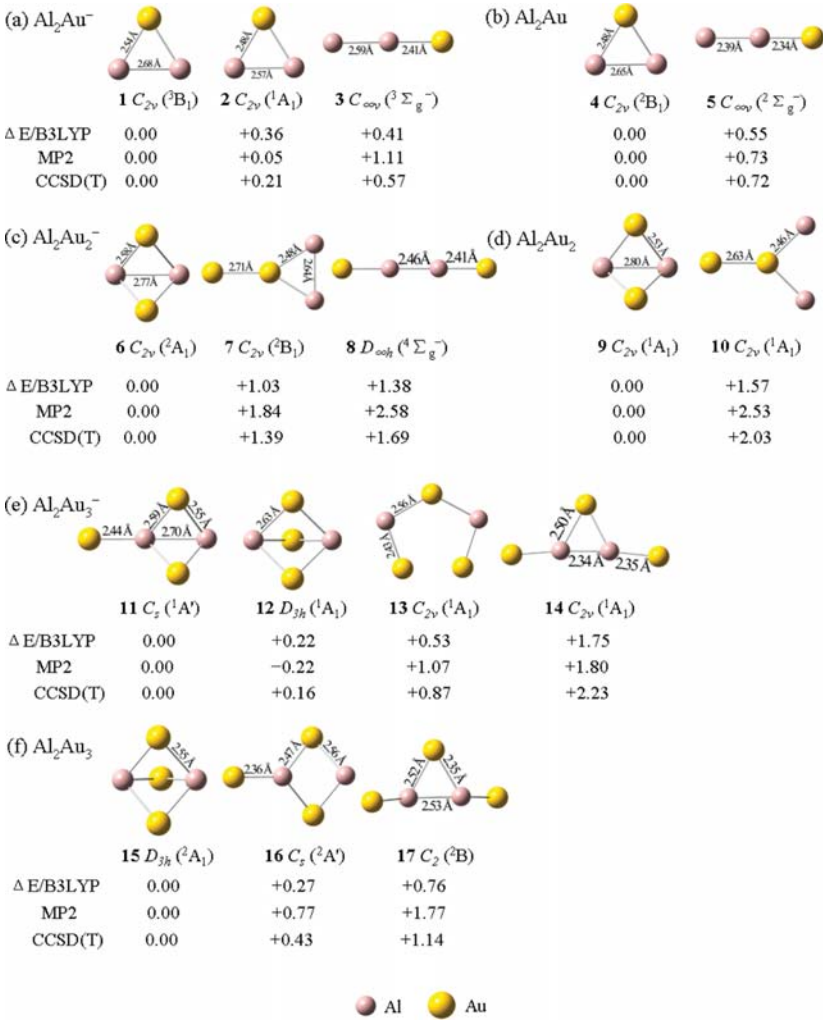

Figure 1. Low-lying isomers of (a) Al_2Au^-, (b) Al_2Au, (c) $Al_2Au_2^-$, (d) Al_2Au_2 (e) $Al_2Au_3^-$, and (f) Al_2Au_3 at B3LYP, with the relative energies ΔE (eV) at B3LYP//B3LYP, MP2//MP2, and CCSD(T)//B3LYP indicated.

results achieved in this work extend the concept of bridging gold to electron-deficient bridging Al−Au−Al and B−Au−Al units and enrich the chemistry of gold, which has wide applications in homogeneous catalyses and metallorganic chemistry.[5−10]

2. THEORETICAL METHODS

Extensive structural searches were performed with use of the DFT-based random structure-generating program (GXYZ).[15] Further structural optimizations, frequency analyses, and natural localized molecular orbital (NLMO) analyses were comparatively conducted on low-lying isomers with use of the hybrid B3LYP method[16] and the second-order Møller−Plesset approach with the frozen core approximation [MP2(FC)].[17] MP2 produced similar ground-state structures and relative energy orders with B3LYP, with slightly different bond parameters. Relative energies for the lowest-lying isomers were further refined by using the coupled cluster method with triple excitations [CCSD(T)][18] at B3LYP structures. The Stuttgart quasi-relativistic pseudopotentials and basis sets augmented with two f-type polarization functions and one g-type polarization function [Stuttgart_rsc_1997_ecp+2f1g (α(f) = 0.498, α(f) = 1.464, and α(g) = 1.218]^{19} were employed for Au with 19 valence electrons. The augmented Dunning's correlation consistent basis set of aug-cc-pvTZ[20] was used for B and Al throughout this work. Adiabatic detachment energies (ADEs) of the anions were calculated as the energy differences between the anions and the corresponding neutrals at their ground-state structures, whereas vertical detachment energies (VDEs) were calculated as the energy differences between the anions and neutrals at the anionic structures. Such a theoretical procedure was proven to be reliable for $SiAu_4^-$, $Si_2Au_x^-$, and $B_7Au_2^-$ in predicting their ground-state structures and analyzing their PES spectra.[6−8] The low-lying isomers obtained are depicted in Figures 1 and 2 with relative energies at B3LYP, MP2, and CCSD(T)//B3LYP levels indicated. The molecular orbital (MO) images and orbital interactions of the Al−Au−Al τ bonds discussed in this work are shown in Figure 3, with the natural atomic charges and Wiberg bond indexes of $Al_2Au_n^{0/-}$ (n = 1−3) tabulated in Table 1 and ADEs and VDEs of the $Al_2Au_n^-$ anions summarized in Table 2. All the calculations in this work were performed with use of Gaussian03.[21]

3. RESULTS AND DISCUSSION

3.1. Geometrical and Electronic Structure. We started from $Al_2Au^{0/-}$, the smallest dialuminum auride, which contains

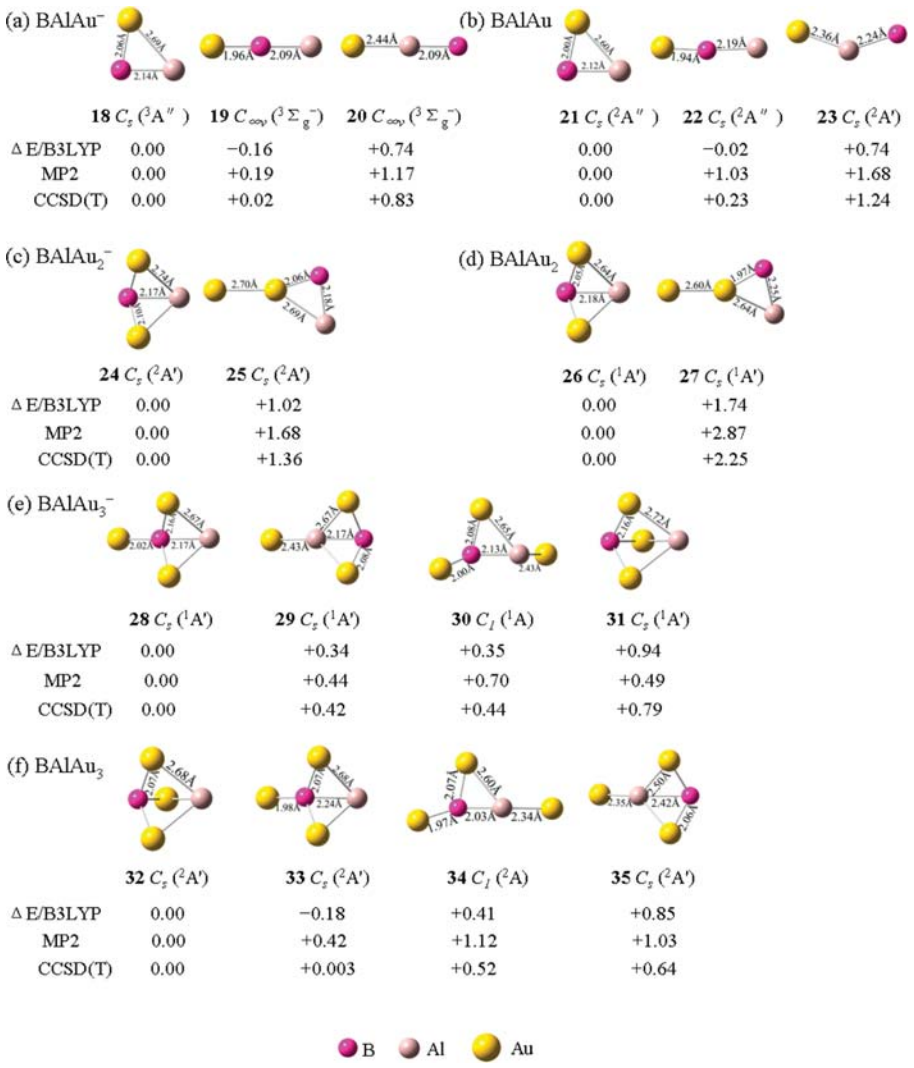

Figure 2. Low-lying isomers of (a) BAlAu$^-$, (b) BAlAu, (c) BAlAu$_2^-$, (d) BAlAu$_2$, (e) BAlAu$_3^-$, and (f) BAlAu$_3$ at B3LYP, with the relative energies ΔE (eV) at B3LYP//B3LYP, MP2//MP2, and CCSD(T)//B3LYP indicated.

a bridging gold. As shown in Figure 1, the triplet Au-bridged C_{2v} Al_2Au^- ($^3B_1$) (**1**) is indeed the ground state of Al_2Au^-: it lies 0.21 and 0.57 eV lower than the singlet Au-bridged C_{2v} Al_2Au^- ($^1A_1$) (**2**) and the triplet linear $C_{\infty v}$ Al_2Au^- ($^3\Sigma_g^-$) (**3**) at CCSD(T), respectively. For neutral structures, the doublet Au-bridged C_{2v} Al_2Au ($^2B_1$) (**4**) (Al(μ-Au)Al), which possesses the same geometry as the V-shaped Al_2H (Al(μ-H)Al),[14] proves to be a local minimum lying 0.72 eV higher than the linear $C_{\infty v}$ Al_2Au (**5**) at CCSD(T) level. The anion $Al_2Au_2^-$ was found to prefer a di-Au-bridged [Al(μ-Au_2)Al]$^-$ structure with a doublet electronic structure. The ground state of the off-planed di-Au-bridged C_{2v} $Al_2Au_2^-$ ($^2A'$) (**6**) is proven to be more stable than the Y-shaped C_{2v} $Al_2Au_2^-$ ($^2B_1$) (**7**) and the quadruplet linear $D_{\infty h}$ $Al_2Au_2^-$ ($^4\Sigma_g^-$) (**8**) (which has two small imaginary frequencies at 18.34i and 17.30i cm^{-1} at B3LYP) at the CCSD(T) level, respectively. For the neutral structure, similar to Al_2H_2 favors a di-H-bridged [Al(μ-H_2)Al] structure, the ground structure of Al_2Au_2 is the di-Au-bridged C_{2v} Al_2Au_2 ($^1A_1$) (**9**), which lies 2.03 eV lower than the Y-shaped C_{2v} Al_2Au_2 ($^1A_1$) (**10**) at the CCSD(T) level. Adding one Au terminally to an Al atom in C_{2v} $Al_2Au_2^-$ ([Al(μ-Au_2)Al]$^-$) ($^2A_1$) (**6**) produces the ground state of di-Au-bridged C_s $Al_2Au_3^-$ [Al(μ-Au_2)Al]Au$^-$ ($^1A'$) (**11**), which proves to be 0.16, 0.87, and 2.23 eV more stable than the tri-Au-bridged D_{3h} $Al_2Au_3^-$ ($^1A_1$) (**12**) (although 0.22 eV less stable than C_s **11** at MP2), the distorted chain C_{2v} $Al_2Au_3^-$ ($^1A_1$) (**13**), and the T-shaped C_{2v} $Al_2Au_3^-$ ($^1A_1$) (**14**) at the CCSD(T) level, respectively. Similar to the tri-H-bridged D_{3h} Al_2H_3 ([Al(μ-H_3)Al]),[14] Al_2Au_3 neutral favors the tri-Au-bridged [Al(μ-Au_3)Al] structure D_{3h} Al_2Au_3 ($^2A_1$) (**15**) over C_s Al_2Au_3 ($^2A'$) (**16**) and C_2 Al_2Au_3 (^2B) (**17**) by 0.43 and 1.14 eV at the CCSD(T) level, respectively.

The hybrid boron−aluminum monoauride was proven to have the ground states of C_s BAuAl$^-$ ($^3A''$) (**18**) for anion and C_s BAuAl ($^2A''$) (**21**) for neutral after the calculation of several isomers (Figure 2). The relative energy difference of the anion isomers **19** and **20** is 0.02 and 0.83 eV, respectively, and 0.23 and 1.24 eV for the neutral isomers **22** and **23** at the CCSD(T) level. Evidently, at the CCSD(T) level, the V-shaped [BAuAl]$^{0/-}$ are more stable than the linear isomers [AlBAu]$^{0/-}$ and significantly more stable than the linear isomers [BAlAu]$^{0/-}$ (although the V-shaped [BAuAl]$^{0/-}$ are

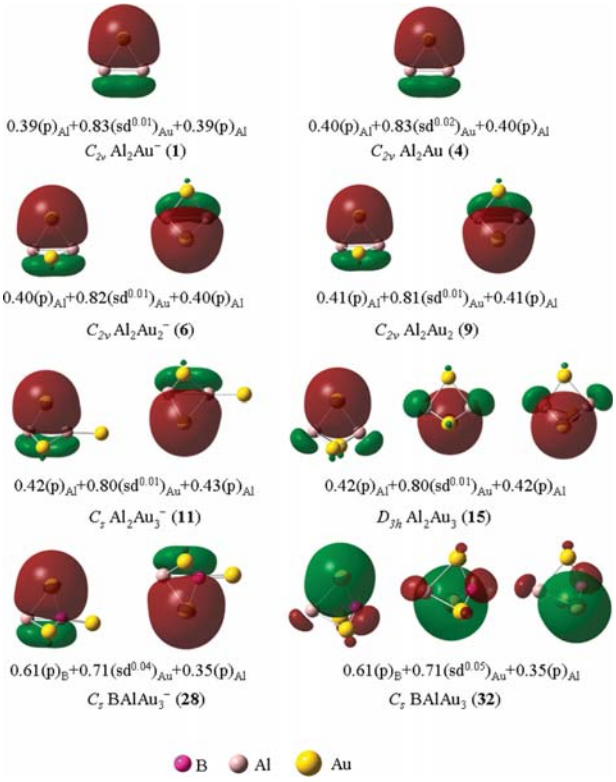

Figure 3. 3D views and orbital interactions of 3c−2e τ bonds in Al_2Au^- (**1**), Al_2Au (**4**), $Al_2Au_2^-$ (**6**), Al_2Au_2 (**9**), $Al_2Au_3^-$ (**11**), Al_2Au_3 (**15**), $BAlAu_3^-$ (**28**), and $BAlAu_3$ (**32**) discussed in this work.

Table 2. Calculated ADEs (eVs) and VDEs (eV) of the Dialuminum Auride Anions at B3LYP and CCSD(T)// B3LYP Levels[a]

	ADE		VDE	
	B3LYP	CCSD(T)	B3LYP	CCSD(T)
C_{2v} Al_2Au^- ($^3B_1$)	1.47 ($^2B_1$)	1.49 ($^2B_1$)	1.49 ($^2B_1$)	1.54 ($^2B_1$)
C_{2v} $Al_2Au_2^-$ ($^2A_1$)	1.45 ($^1A_1$)	1.40 ($^1A_1$)	1.47 (^1A)	1.46 (^1A)
C_s $Al_2Au_3^-$ ($^1A'$)	2.15 ($^2A_1$)	1.97 ($^2A_1$)	2.70 ($^2A'$)	2.73 ($^2A'$)

[a]ADEs of the anions are equivalent to the electron affinities of the corresponding neutrals.

less stable than the linear isomers $[AlBAu]^{0/-}$ at the DFT level (Figure 2)). C_s BAuAl ($^2A''$) (**21**) has a different geometry from the ground-state linear AlBH.[22] For hybrid boron−aluminum diaurides, the C_s $BAlAu_2^-$ ($^2A'$) (**24**) is 1.36 eV more stable than the Y-shaped $BAlAu_2^-$ (**25**) ($^2A'$), whereas the C_s $BAlAu_2$ ($^1A'$) (**26**) lies 2.25 eV lower than the distorted Y-shaped $BAlAu_2$ (**27**) ($^1A'$) at the CCSD(T) level. Similar to the structure mode of C_s $Al_2Au_3^-$ $[Al(\mu\text{-}Au_2)Al]Au^-$ ($^1A'$) (**11**), the di-Au-bridged C_s $[Al(\mu\text{-}Au_2)BAu]^-$ ($^1A'$) (**28**) appears to lie 0.42, 0.44, and 0.79 eV lower than the C_s $BAlAu_3^-$ (**29**), C_1 $BAlAu_3^-$ (**30**) and C_s $BAlAu_3^-$ (**31**) at CCSD(T), respectively. The global minimum of $BAlAu_3$ neutral turned out to be C_s $[Al(\mu\text{-}Au_3)B]$ ($^2A_1$) (**32**), which contains three B−Au−Al bridges. The di-Au-bridged C_s $[Al(\mu\text{-}Au_2)BAu]$ ($^2A'$) (**33**), which has the same calculated parameters as the **32** isomer, lies only slightly higher, 0.003 eV, than C_s **32** at the CCSD(T) level (although 0.18 eV lower than C_s **32** at B3LYP and 0.42 eV higher than C_s **32** at MP2).

We note that the geometry and electric structures of the dialuminum aurides $[Al_2Au_n]$ (n = 1−3) are nearly identical with those of the dialuminum hydride (Al_2H_n) molecules.[14]

Table 1. Calculated Natural Atomic Charges (q/lel), Wiberg Bond Indexes (WBI), and Total Atomic Bond Orders (WBI_{Al} and WBI_{Au}) of the Au-Bridged $Al_2Au_n^{0/-}$ and $BAlAu_n^-$ Clusters at the B3LYP Level[a]

	q_{Al}	q_B	$q_{Au(b)}$	WBI		WBI_{Al}	$WBI_{Au(b)}$	WBI_B
C_{2v} Al_2Au^- (**1**)	−0.34		−0.33	Al−Al	0.98	1.51	1.05	
				Al−Au(b)	0.53			
C_{2v} Al_2Au (**4**)	0.13		−0.27	Al−Al	0.99	1.55	1.12	
				Al−Au(b)	0.56			
C_s $BAlAu^-$ (**18**)	0.05	−0.94	−0.10	B−Al	1.15	1.55	1.22	2.05
				B−Au	0.90			
				Al−Au(b)	0.33			
C_{2v} $Al_2Au_2^-$ (**6**)	−0.22		−0.28	Al−Al	0.85	1.89	1.08	
				Al−Au(b)	0.52			
C_{2v} Al_2Au_2 (**9**)	0.23		−0.23	Al−Al	0.77	1.88	1.14	
				Al−Au(b)	0.55			
C_s $BAlAu_2^-$ (**24**)	0.17	−1.11	−0.03	B−Al	1.13	1.75	1.24	2.86
				B−Au(b)	0.87			
				Al−Au(b)	0.31			
C_s $Al_2Au_3^-$ (**11**)	−0.10		−0.22	Al−Al′	1.08	2.32[b]		
	−0.09			Al−Au(b)	0.54			
				Al′−Au(b)	0.53	2.90[c]		
				Al′- Au(t)	0.76			
D_{3h} Al_2Au_3(**15**)	0.17		−0.12	Al−Al	0.45	1.93	1.10	
				Al−Au(b)	0.49			
C_s $BAlAu_3^-$ (**28**)	0.28	−1.32	0.02	B−Al	1.08	1.91	1.28	3.69
				B−Au	0.83			
				Al−Au	0.33			

[a]Au (b) represents bridging Au atom and Al′ represents the Al atom connected with terminal Au atom in C_s $Al_2Au_3^-$ (**21**). [b]For Al. [c]For Al′.

dx.doi.org/10.1021/jp4026656 | J. Phys. Chem. A 2013, 117, 5178−5183

However, the geometries of the hybrid boron−aluminum aurides [$BAlAu_n$] (n = 1−3) are different from those of the hybrid boron−aluminum hydride ($BAlH_n$) molecules.[22] There is very little geometry change between the ions and the neutrals of $Al_2Au_n^{0/-}$ or $BAlAu_n^{0/-}$ (n = 1−2), except for $Al_2Au_3^{0/-}$ and $BAlAu_3^{0/-}$.

3.2. Bonding Considertion. In both C_{2v} Al_2Au^- ($^3B_1$) (**1**) and Al_2Au ($^2B_1$) (**4**), Au 6s overlaps with one of the two half-filled π_u orbitals of Al_2 ($^3\Sigma_g^-$) to form the Al−Au−Al τ interactions. The Wiberg bond orders of WBI_{Al-Au} = 0.53 in **1** and WBI_{Al-Au} = 0.56 in **4**, respectively, well support the existence of the τ bonds in them, while the bond orders of WBI_{Al-Al} = 0.98 in **1** and WBI_{Al-Al} = 0.99 in **4** as well as the bond lengths r_{Al-Al} = 2.68 Å in **1** and r_{Al-Al} = 2.65 Å in **4** exhibit no significant changes. Detailed NLMO analyses quantitatively reveal the existence of a bridging Al−Au−Al τ bond in both C_{2v} Al_2Au^- (**1**) and Al_2Au (**4**), as clearly shown in their 3c-2e orbital images and orbital interactions in Figure 3. With the orbital combination of $\tau_{Al-Au-Al} = 0.39(sp^{80.3})_{Al} + 0.83(sd^{0.01})_{Au} + 0.39(sp^{80.3})_{Al}$ and the corresponding atomic contribution of 15%Al + 70%Au + 15%Al for the τ bond in C_{2v} Al_2Au^- (**1**), Au 6s and Au 5d contribute 98.4% and 1.3% to the Au-based orbital, respectively, whereas Al 3p and Al 3s contribute 97.7% and 1.2% to the Al-based orbital, respectively. Evidently, Au 6s and Al 3p make the main contribution to the Al−Au−Al bridging bond in C_{2v} Al_2Au^-, well in agreement with the qualitative discussion presented above. Compared with the composition of the B−Au−B 3c-2e bond in C_{2v} B_2Au^-,[11] Au 6s makes a larger contribution to the Au-based orbital in C_{2v} Al_2Au^- than in C_{2v} B_2Au^-. However, given the strong relativistic effects of Au, the 1.3% contribution from Au 5d is not negligible. Thus, the 3c-2e bond of C_{2v} Al_2Au^- can be practically approximated as $\tau_{Al-Au-Al} = 0.39(p)_{Al} + 0.83(sd^{0.01})_{Au} + 0.39(p)_{Al}$. Similar to C_{2v} Al_2Au^- (**1**), neutral C_{2v} Al_2Au (**4**) possesses a $\tau_{Al-Au-Al}$ bond with the orbital combination of $\tau_{Al-Au-Al} = 0.40(p)_{Al} + 0.83(sd^{0.02})_{Au} + 0.40(p)_{Al}$.

Population analysis demonstrates that the most stable structures of the hybrid boron−aluminum monoaurides C_s $BAuAl^{0/-}$ and the dialuminum aurides C_{2v} $Al_2Au^{0/-}$ exhibit different bonding patterns despite the fact that they have similar structures. In other words, a bridging B−Au−Al τ bond does not exist in both C_s $BAuAl^-$ (**18**) and C_s BAuAl (**21**). In C_s $BAuAl^-$ ($^3A''$) (**18**), the bond has a length of r_{B-Au} = 2.06 Å, r_{Al-Au} = 2.69 Å, and r_{B-Al} = 2.14 Å with corresponding bond orders of WBI_{B-Au} = 0.90, WBI_{Al-Au} = 0.33, and WBI_{B-Al} = 1.15, respectively. Both B−Al and B−Au have considerably stronger electronic interaction than Al−Au. The atomic charges of q_B = −0.94 |e|, q_{Al} = 0.05 |e|, and q_{Au}=−0.10 |e| indicate that the extra electron of the anion is totally localized in the B−Au bond, thus preventing the formation of the B−Au−Al τ bonding in C_s $BAuAl^-$ (**18**). A similar situation exists in C_s BAuAl (**21**).

As for di-Au-bridged C_{2v} $Al_2Au_2^-$ (**6**), its Al−Al and Al−Au bonds have bond lengths of 2.77 and 2.58 Å (Figure 1) with corresponding Wiberg bond orders of 0.85 and 0.52 (Table 1), respectively. Atomic charges of q_{Al} = −0.22 |e| and q_{Au} = −0.28 |e| in **6** indicate that the additional electron of the anion is distributed in the whole molecule. Detailed NLMO analyses quantitatively reveal the existence of two bridging Al−Au−Al τ bonds both in C_{2v} $Al_2Au_2^-$ (**6**) and C_{2v} Al_2Au_2 (**9**). With the orbital combination of $\tau_{Al-Au-Al} = 0.40(p)_{Al} + 0.82(sd^{0.01})_{Au} + 0.40(p)_{Al}$ and the corresponding atomic contribution of 16%Al + 68%Au + 16%Al for the τ bond in C_{2v} $Al_2Au_2^-$ (**6**), Au 6s and Au 5d contribute 98.8% and 0.97% to the Au-based orbital, respectively, whereas Al 3p and Al 3s contribute 97.4% and 1.3% to the Al-based orbital, respectively. Consistent with C_{2v} Al_2Au^-, Au 6s and Al 3p make major contributions to the Al−Au−Al bridging bond in C_{2v} $Al_2Au_2^-$, which agrees with the qualitative discussion presented above. As a local minimum, neutral C_{2v} Al_2Au_2 (**9**) possesses a 3c-2e bond $\tau_{Al-Au-Al} = 0.41(p)_{Al} + 0.81(sd^{0.01})_{Au} + 0.41(p)_{Al}$, which is similar to that of C_{2v} $Al_2Au_2^-$ (**6**).

No bridging B−Au−Al τ bond exists in both C_s $BAuAl_2^-$ (**24**) and C_s $BAuAl_2$ (**26**), similar to the hybrid boron−aluminum monoauride C_s $BAuAl^-$ (**18**) and C_s BAuAl (**21**). The distance of Al−Au increased from 2.58 Å in **6** to 2.74 Å in **24**, and the bond order decreased from 0.52 in **6** to 0.31 in **24**, implying that **6** and **24** have different electronic structures. The B atoms in C_s $BAlAu_2^-$ ($^2A'$) (**24**) have bond lengths of r_{B-Au} = 2.10 Å and r_{B-Al} = 2.17 Å with corresponding bond orders of 0.87 and 1.13, respectively. The atomic charges of q_B = −1.11|e|, q_{Au} = −0.03 |e|, and q_{Al} = 0.17 |e| in **24** indicate that the extra electron of the anion is totally localized in the B−Au bond and the B−Au−Al τ bonding mode does not exist in C_s $BAuAl_2^-$ (**24**). Thus, B−Au has a significantly stronger electronic interaction than Al−Au in C_s $BAuAl_2^-$ (**24**). As a local minimum, neutral C_s $BAuAl_2$ (**26**) possesses an electronic structure similar to that of C_s $BAuAl_2^-$ (**24**).

The 3c-2e $\tau_{Al-Au-Al}$ bond in C_s $Al_2Au_3^-$ (**11**) possesses the orbital combination of $\tau_{Al-Au-Al} = 0.42(p)_{Al} + 0.80(sd^{0.01})Au + 0.43(p)_{Al}$. The two Al atoms in C_s $Al_2Au_3^-$ form an Al−Al σ bond with r_{Al-Al} = 2.70 Å with corresponding bond orders of 1.08 (Table 1), whereas the Au $6s^1$ electron and the additional electron of the anion form the bridging interaction with $r_{Al-Au(b)}$ = 2.55−2.59 Å and corresponding bond orders of 0.53−0.54. The terminal (t) bond in **11** has a bond length of 2.44 Å with a corresponding bond order of 0.76. D_{3h} Al_2Au_3 (**15**) possesses three equivalent $\tau_{Al-Au-Al}$ bonds with the orbital combination of $\tau_{Al-Au-Al} = 0.42(p)_{Al} + 0.80(sd^{0.01})_{Au} + 0.42(p)_{Al}$.

Unlike the bonding pattern of $BAlAu^{0/-}$ and $BAlAu_2^{0/-}$, $BAlAu_3^{0/-}$ possess a bridging B−Au−Al τ bond in both ground states of C_s $BAlAu_3^-$ (**28**) ($^1A'$) and C_s $BAlAu_3$ (**32**) ($^2A'$), which have a similar structure mode and bonding pattern as C_s $Al_2Au_3^-$ (**11**) and D_{3h} Al_2Au_3 (**15**). C_s [Al(μ-Au_2)BAu]$^-$ ($^1A'$) (**28**) with r_{B-Al} = 2.17 Å possesses a 3c-2e bond of $\tau_{Al-Au-Al} = 0.61(p)_B + 0.71(sd^{0.04})_{Au} + 0.35(p)_{Al}$. As a local minimum, neutral C_s $BAlAu_3$ ([Al(μ-Au_3)B]) ($^2A'$) (**32**) possesses similar three-center interactions as C_s $BAlAu_3^-$ ([Al(μ-Au_2)BAu]$^-$) ($^1A'$) (**28**). Notably, in the orbital combinations of the bridging bonds in $BAlAu_3^{0/-}$ clusters, Al has slightly lower orbital coefficients (0.35) and therefore less contribution to the multicenter interactions than B (0.61).

$Al_2Au_n^{0/-}$ (n = 1−3) are proven to possess a Al−Au−Al τ bond and $BAlAu_3^{0/-}$ was demonstrated to possess a B−Au−Al τ bond (vide supra). However, no bridging B−Au−Al τ bond exists in $BAlAu_n^{0/-}$ (n = 1−2). Au 6s provides the main contribution to the Au-based orbital in bridging Al−Au−Al or B−Au−Al units, which reflects the relative effect of gold. In addition, B makes more contribution than Al in the orbital combinations of B−Au−Al τ bond in $BAlAu_3^{0/-}$. Considering the similar electronegativity of gold (2.4) and hydrogen (2.2), it is interesting to note that the atomic charges of q_{Au} = −0.33 to −0.12 |e| in $Al_2Au_n^{0/-}$ (n = 1−3), perhaps predicting that the isolobal analogy between Au and H exists in the [$AlAu_n$] series of molecules.

3.3. Electron Detachment Energies. As shown in Table 2, B3LYP and CCSD(T) methods produced consistent one-electron detachment energies for $Al_2Au_n^-$ (n = 1−3) anions, making them possible to characterize in PES experiments. C_{2v} Al_2Au^- (**1**) anion has calculated ADE = 1.49 eV and VDE = 1.54 eV at the CCSD(T)//B3LYP level, whereas C_{2v} $Al_2Au_2^-$ (**6**) anion has calculated ADE = 1.40 eV and VDE = 1.46 eV at the same level. The small ADE−VDE differences (0.05−0.06 eV) agree with the minor structural relaxation from the C_{2v} anion and C_{2v} neutral. When one electron is detached, a significant structural change occurs from C_s $Al_2Au_3^-$ (**11**) to D_{3h} Al_2Au_3 (**15**). This prediction agrees with the huge energy difference (0.76 eV) between the calculated ADE (1.97 eV) and VDE (2.73 eV) at the CCSD(T) level. The electron binding energies of these anions fall within the energy range of the conventional excitation laser (266 nm, 4.661 eV) in PES measurements.

4. SUMMARY

We presented a geometrical and electronic structure analysis for electron-deficient $Al_2Au_n^{0/-}$ (n = 1−3) and $BAlAu_n^{0/-}$ (n = 1−3) clusters at both DFT and wave function theory levels. Aluminum aurides $Al_2Au_n^{0/-}$ (n = 1−3) are predicted to possess bridging gold atoms, which are all proven to possess a Al−Au−Al τ bond, whereas only $BAlAu_3^{0/-}$ was demonstrated to possess a B−Au−Al τ bond in hybrid boron−aluminum aurides $BAlAu_n^{0/-}$ (n = 1−3). The neutral Al_2Au_n [Al(μ-Au_n)Al] (n = 1−3) have similar geometrical and electric structures as Al_2H_n [Al(μ-H_n)Al] (n = 1−3). B has more contributions to the multicenter interactions than Al in the orbital combinations of the bridging bonds in $BAlAu_3^{0/-}$ clusters. Detailed orbital analysis indicates that Au 6s and Au 5d respectively contribute 98%−99% and 1%−2% to the Au-based orbitals in bridging Al−Au−Al or B−Au−Al units, partially reflecting the relativistic effect of gold. B−Al and B−Au exhibit a significantly stronger electronic interaction than Al−Au in $BAlAu^{0/-}$ and $BAlAu_2^{0/-}$, which do not possess a bridging gold. The one-electron detachment energies of dialuminum auride clusters $Al_2Au_n^-$ (n = 1−3) with ADE (1.40 −1.97 eV) and VDE (1.46−2.73 eV) were calculated at ab initio levels, which may facilitate their future experimental characterization. Bridging gold addressed in this work provides an interesting bonding mode for $AlAu_n$ and $BAlAu_n$ electron-deficient systems and may aid in designing new masteries and catalysts with highly dispersed Au atoms.

■ AUTHOR INFORMATION

Corresponding Author

*E-mail: yaowenzhi-1982@163.com.

Notes

The authors declare no competing financial interest.

■ ACKNOWLEDGMENTS

This work was financially supported by the North China University of Water Conservancy and Electric Power High-level experts Scientific Research foundation (No. 201114)

■ REFERENCES

(1) Pyykko, P. *Angew. Chem., Int. Ed.* **2002**, *41*, 3573 and references therein..

(2) Cotton, F. A.; Wikinson, G.; Murillo, C. A.; Bochmann, M. *Advances in Inorganic Chemistry*, 6th ed.; Wiley: New York, NY, 1999.

(3) Schwarz, H. *Angew Chem., Int. Ed.* **2003**, *42*, 4442 and references therein..

(4) Gagliardi, L. *J. Am. Chem. Soc.* **2003**, *125*, 7504.

(5) (a) Hall, K. P.; Mingos, D. M. P. *Prog. Inorg. Chem.* **1984**, *32*, 237. (b) Lauher, J. W.; Wald, K. *J. Am. Chem. Soc.* **1981**, *103*, 7648. (c) Burdett, J. K.; Eisentein, O.; Schweizer, W. B. *Inorg. Chem.* **1994**, *33*, 3261.

(6) Kiran, B.; Li, X.; Zhai, H. J.; Cui, L. F.; Wang, L. S. *Angew Chem., Int. Ed.* **2004**, *43*, 2125.

(7) (a) Li, X.; Kiran, B.; Wang, L. S. *J. Phys. Chem. A* **2005**, *109*, 4366. (b) Kiran, B.; Li, X.; Zhai, H. J.; Wang, L. S. *J. Chem. Phys.* **2006**, *125*, 133204.

(8) Zhai, H. J.; Wang, L. S.; Zubarev, D. Y.; Boldyrev, A. I. *J. Phys. Chem. A* **2006**, *110*, 1689.

(9) Zubarev, D. Y.; Li, J.; Wang, L. S.; Boldyrev, A. I. *Inorg. Chem.* **2006**, *45*, 5269.

(10) Pyykko, P.; Zhao, Y. *Chem. Phys. Lett.* **1991**, *117*, 103.

(11) Yao, W. Z.; Li, D. Z.; Li, S. D. *J. Comput. Chem.* **2011**, *32*, 218.

(12) Li, D. Z.; Li, S. D. *Int. J. Quantum Chem.* **2011**, *111*, 4418.

(13) Yao, W. Z; Yao, J. B; Li, S. D. *Chin. J. Struct. Chem.* **2012**, *31*, 1549.

(14) Liu, J.; Aeschleman, J.; Rajan, L. M.; Che, C.; Ge, Q. In *Materials Issues in A Hydrogen Economy*, Jena, P., Kandalam, A., Sun, Q., Eds.; World Scientific Publishing Co. Ptc. Ltd: Singapore, 2009, p234.

(15) Lu, H.-G. In GXYZ Ver. 1.0, A Random Cartesian Coordinates Generating Program; Shanxi University: Taiyuan, China, 2008.

(16) (a) Becke, A. D. *J. Chem. Phys.* **1993**, *98*, 5648. (b) Lee, C.; Yang, W.; Parr, R. G. *Phys. Rev. B* **1988**, *37*, 785.

(17) (a) Head-Gordon, M.; Pople, J. A.; Frisch, M. *J. Chem. Phys. Lett.* **1988**, *153*, 503. (b) Frisch, M. J.; Head-Gordon, M.; Pople, J. A. *Chem. Phys. Lett.* **1990**, *166*, 275. (c) Frisch, M. J.; Head-Gordon, M.; Pople, J. A. *Chem. Phys. Lett.* **1990**, *166*, 281. (d) Head-Gordon, M.; Head-Gordon, T. *Chem. Phys. Lett.* **1994**, *220*, 122. (e) Saebo, S.; Almlof, J. *Chem. Phys. Lett.* **1989**, *154*, 83.

(18) (a) Cizek, J. *Adv. Chem. Phys.* **1969**, *14*, 35. (b) Scuseria, G. E.; Schaefer, H. F. *J. Chem. Phys.* **1989**, *90*, 3700. (c) Pople, J. A.; Head-Gordon, M.; Raghavachari, K. *J. Chem. Phys.* **1987**, *87*, 5968.

(19) (a) Dolg, M.; Wedig, U.; Stoll, H.; Preuss, H. *J. Chem. Phys.* **1987**, *86*, 866. (b) Martin, J. M. L.; Sundermann, A. *J. Chem. Phys.* **2001**, *114*, 3408.

(20) Kendall, R. A.; Dunning, T. H.; Harrison, R. J. *J. Chem. Phys.* **1992**, *96*, 6796.

(21) Frisch, M. J. et al. *Gaussian 03*, revision, A.1; Gaussian, Inc.: Pittsburgh, PA, 2003.

(22) Gilbert, J. M.; Charles, W. B.; Mendel, T.; Joe, F. *J. Phys. Chem.* **1990**, *94*, 6996.